On a meso-elastoplastic constitutive equation with application to deformation-induced anisotropy of a polycrystalline aggregate

HONG-QIU LIU (BEIJING) and K. HUTTER (DARMSTADT)

BASED ON A 3-D MESO-MATERIAL MODEL of a polycrystalline aggregate, an elastoplastic constitutive equation for finite deformation is derived. The emphasis is focused on discussing the anisotropy induced by the heterogeneity in the material properties due to a complex deformation history, as well as re-orientation of the crystals or the variation of the micro-structure due to finite deformation. The theoretical predictions are in good agreement with experimental results.

1. Introduction

POLYCRYSTALLINE MATERIALS, such as metals, rock or ice, display distinct anisotropy when they undergo complex deformation processes, like multistage rolling and stretching connected with heat treatment of the material during the manufacturing process or large shear under creep. At greater depths in the Antarctic or Greenland ice caps, glacier ice gives rise to re-crystallization due to extreme stresses consisting of a combination of pressure and shear so as to result in anisotropy of polycrystalline ice (THORSTEINSSON [1]). Therefore, much attention is devoted to the deformation or stress-induced anisotropy in polycrystalline materials. Because the anisotropy induced by plastic deformation history in a polycrystalline material is load-dependent and thus very complicated, SZCZEPIŃSKI [2] proposed a theoretical description of the deformation-induced anisotropy, which is treated as an existing property of the material, without connecting it with the previous deformation history, and discussed the corresponding experimental determination of the coefficients of plastic anisotropy (SOCHA and SZCZEPIŃSKI [3]). This description involves the introduction of structure tensors. DAFALIAS [4] applied the representation theorems for isotropic functions in conjunction with the concept of tensorial structure variables to provide explicit forms of constitutive relations for the plastic spin, and developed a general constitutive formulation employing multiple constitutive and plastic spins for the tensorial internal variables (DAFALIAS [5]). RANIECKI and MRÓZ [6] proposed that the texture orientation can be specified by a rigidly rotating triad; the plastic spin is then the difference of the material and texture spins.

Many factors can cause anisotropy of a polycrystalline material. Generally, in macro-experiments one measures the anisotropy induced by the heterogeneity in the material properties of a body undergoing some deformation history (SZCZEPIŃSKI [7]). With the development of micro-observation techniques, the

micro-experiment is focused on the re-orientation of crystals or the variation of micro-structure (Steinemann [8]). Consequently, theoretical descriptions of the orientation of crystals or the micro-structure of the material became feasible. Ribe [9]) Van der Giessen [10] and Svendsen and Hutter [11] applied the concept of an orientation distribution function (ODF) to modelling induced anisotropy in polycrystalline materials. Lipiński et al. [12] had let 100 ellipsoidal inclusions replace FCC crystal grains as a polycrystalline aggregate and analysed the variation of grain orientation and their influence on the macro-stress distribution by a statistical approach.

In fact, a practical polycrystalline material consists of hundreds of thousands of irregular single crystals. Its micro-structure is so complicated that we can hardly describe it clearly, let alone its evolution during deformation. Since polycrystalline ice or metal are aggregates of randomly oriented grains of single crystals, they can be considered as initially isotropic materials. Generally, the bulk mechanical response of the polycrystalline aggregate is the average result of interactions between various micro-structures, in which some physical actions observed on the microscale have little influence on the macro-response of the material so that they can be neglected. Experimental results show that the sliding occurring between grains is mainly a plastic deformation mechanism of polycrystalline materials, while the deformation of the grains is very small. Based on these experimental facts, equivalent slip systems are introduced, which are basic components distributed homogeneously in the 3-D space. Thus a meso-material model is composed of the equivalent slip systems and elastic grains. With the aid of the model under small deformation, Liang et al. [13] and Liu and Liang [14] discussed the active hardening, latent hardening and Bauschinger effect, and predicted the evolution of subsequent yield surfaces and stress-strain responses under complex and cyclic loading, respectively. Here, a meso-elastoplastic constitutive equation is derived for finite deformation. Emphasis is laid on discussing the deformation-induced anisotropy and its evolution due to the variation of the properties, and re-orientation of the equivalent slip systems due to the deformation history of the polycrystalline material. Numerical results are presented and compared with the experimental data (Szczepiński [7]). The re-orientation or re-crystallization of polycrystalline ice induced by creep deformation will be discussed in later papers.

2. Fundamental assumptions of a material model

The polycrystalline material is assumed to consist of a vast number of micro-grains. Sliding is heterogeneously and randomly distributed in the 3-D space; it occurs principally between grains or on their boundaries, while the deformation of the grains is usually small. Basing on various experimental observations, we postulate several basic phenomenological features of polycrystalline aggregates

in deformation and attempt to build a material model that has characteristics consistent with the material and can predict the behavior of the material during complex loadings. Here, we assume that

1. *The sliding between grains is the only plastic deformation mechanism. Then, a basic component of a material model is an equivalent slip system*, which is composed of many intermittent micro-slidings in a direction m on slip planes of grains with a unit normal vector n. *The sliding driving stress τ is the objective scalar equal to the macro resolved shear stress associated with directions* m *and* n:

$$(2.1) \qquad \tau = T : m \otimes n = T : P,$$

where T is the Cauchy stress, and

$$(2.2) \qquad P = \frac{1}{2}(m \otimes n + n \otimes m)$$

is the symmetric orientation tensor of the slip system. The sliding rate is work conjugate with the resolved shear stress rate of the slip system. The relation between them is determined by the *slip hardening law* proposed by LIANG *et al.* [13]. Because polycrystalline aggregates can be considered as initially homogeneous and isotropic, *equivalent slip systems are homogeneously distributed and oriented in the* 3-D *space*.

2. The deformation of grains is small, so that *grains in the aggregate are supposed to form an isotropic elastic medium*. Thus, its constitutive equation may be stated in the form

$$(2.3) \qquad \check{T} = IK_g : D_g,$$

where $\check{T}$ is the Jaumann rate of the stress T, i.e.

$$(2.4) \qquad \check{T} = \dot{T} - W \cdot T + T \cdot W + tr(D)T,$$

D the overall strain rate, D_g the strain rate of the grains and IK_g the elastic stiffness tensor of the grains.

3. *The overall strain rate of the aggregate is the sum of the strain rates of the grains* D_g *and the slip system,* D_s, i.e.,

$$(2.5) \qquad D = D_g + D_s,$$

where D_s is the strain rate produced by sliding.

4. *The slip systems and their orientations deform as material lines and surfaces, respectively*. Therefore, the rates of unit sliding direction m and normal vector n are derived, respectively, as

$$(2.6) \qquad \begin{aligned} \dot{m} &= L \cdot m - (m \otimes m : D)m, \\ \dot{n} &= -n \cdot L + (n \otimes n : D)n, \end{aligned}$$

where the deformation velocity gradient $\mathbf{L} = \text{grad}\,\mathbf{v}$ of the aggregate is

(2.7) $\mathbf{L} = \mathbf{D} + \mathbf{W}$.

With these, the rate of orientation tensor of a slip system is expressible as

(2.8) $\dot{\mathbf{P}} = \mathbf{D}\cdot\mathbf{R} - \mathbf{R}\cdot\mathbf{D} - \mathbf{P}\cdot\mathbf{W} + \mathbf{W}\cdot\mathbf{P} + \mathbf{P}\otimes(\mathbf{n}\otimes\mathbf{n} - \mathbf{m}\otimes\mathbf{m}):\mathbf{D}$,

where $\mathbf{W} = \text{skw}\,\mathbf{L}$ is the spin tensor and $\mathbf{R} = \dfrac{1}{2}(\mathbf{m}\otimes\mathbf{n} - \mathbf{n}\otimes\mathbf{m})$ the antisymmetric orientation tensor of the slip system.

It is noteworthy that two forms of the tensor products, $\otimes$ and $\bowtie$, defined, respectively, as

(2.9) $(\mathbf{A}\otimes\mathbf{B})_{ijkl} = (A)_{ij}\,(B)_{kl}$ and $(\mathbf{A}\bowtie\mathbf{B})_{ijkl} = A_{ik}B_{jl}$

are used in this paper.

3. Elastoplastic constitutive relation of the aggregate

In the current configuration, the overall rate of work dissipated in a unit volumetric element is equal to the sum of the powers dissipated by all active slip systems

(3.1) $\dot{w}_s = \mathbf{T}:\mathbf{D}_s = \mathbf{T}:\dfrac{1}{J}\displaystyle\int_{\Omega}\int_{\psi}\dot{\gamma}\,\mathbf{P}\,d\Omega\,d\psi$,

where $J = \det\mathbf{F}$ is the Jacobian of the deformation gradient $\mathbf{F}$ and $\dot{\gamma}$ is the equivalent sliding rate with normal vector $\mathbf{n}$ within a solid angle $d\Omega$, and slip direction $\mathbf{m}$ within a plane angle $d\psi$. Therefore the strain rate $\mathbf{D}_s$ produced by sliding is obtained as

(3.2) $\mathbf{D}_s = \dfrac{1}{J}\displaystyle\int_{\Omega}\int_{\psi}\dot{\gamma}\,\mathbf{P}\,d\Omega\,d\psi$.

According to the slip hardening law proposed by LIANG *et al.* [13], the sliding rate is contributed by *active hardening* and *latent hardening*, respectively, i.e.,

(3.3) $\dot{\gamma} = \dfrac{1}{h}(\dot{\tau} - \chi\mathbf{P}:\mathbf{D}_s)$,

where h is the active hardening modulus, while χ is the latent hardening modulus. Using Eqs. (2.4) and (2.8), the resolved shear stress rate Eq. (2.1) on the current configuration becomes

(3.4) $\dot{\tau} = \mathbf{P}:\dot{\mathbf{T}} + \dot{\mathbf{P}}:\mathbf{T}$

               $= \mathbf{P}:\dot{\mathbf{T}} + [\mathbf{R}\cdot\mathbf{T} - \mathbf{T}\cdot\mathbf{R} + (\mathbf{T}:\mathbf{P})(\mathbf{n}\otimes\mathbf{n} - \mathbf{m}\otimes\mathbf{m} - \mathbf{I})]:\mathbf{D}$.

Substituting Eqs. (3.3) and (3.4) into Eq. (3.2) and using Eq. (2.5) yields

$$(3.5) \qquad \mathbf{D} - \mathbf{D}_g = \left[\frac{1}{J} \int_\Omega \int_\psi \frac{1}{h} (\mathbf{P} \otimes \mathbf{P}) \, d\Omega \, d\Psi \right] : \check{\mathbf{T}}$$

$$- \left[\frac{1}{J} \int_\Omega \int_\psi \frac{1}{h} \chi \mathbf{P} \otimes \mathbf{P} \, d\Omega \, d\Psi \right] : (\mathbf{D} - \mathbf{D}_g)$$

$$+ \left[\frac{1}{J} \int_\Omega \int_\psi \frac{1}{h} \{ \mathbf{P} \otimes [\mathbf{R} \cdot \mathbf{T} - \mathbf{T} \cdot \mathbf{R} + (\mathbf{T} : \mathbf{P})(\mathbf{n} \otimes \mathbf{n} - \mathbf{m} \otimes \mathbf{m} - \mathbf{I})] \} \, d\Omega \, d\Psi \right] : \mathbf{D}.$$

Rewriting the above equation, thereby using Eq. (2.3) in the form $\mathbf{D}_g = \mathbf{IK}_g^{-1} : \check{\mathbf{T}}$, the explicit form of an elastoplastic constitutive equation for finite deformation takes the form

$$(3.6) \qquad \left[\mathbf{I} \bowtie \mathbf{I} + \frac{1}{J} \int_\Omega \int_\psi \frac{1}{h} [\chi \mathbf{P} \otimes \mathbf{P} - \mathbf{P} \otimes (\mathbf{R} \cdot \mathbf{T} - \mathbf{T} \cdot \mathbf{R}) \right.$$

$$\left. - (\mathbf{P} : \mathbf{T}) \mathbf{P} \otimes (\mathbf{n} \otimes \mathbf{n} - \mathbf{m} \otimes \mathbf{m} - \mathbf{I})] d\Omega \, d\Psi \right] : \mathbf{D}$$

$$= \left[\mathbf{K}_g^{-1} + \frac{1}{J} \int_\Omega \int_\psi \frac{1}{h} (\mathbf{P} \otimes \mathbf{P} + \chi \mathbf{P} \otimes \mathbf{P} : \mathbf{K}_g^{-1}) \, d\Omega \, d\Psi \right] : \check{\mathbf{T}}.$$

Under small deformation, this simplifies [13] to

$$(3.7) \qquad \left[\mathbf{I} \bowtie \mathbf{I} + \int_\Omega \int_\psi \frac{\chi}{h} \mathbf{P} \otimes \mathbf{P} \, d\Omega \, d\Psi \right] : \mathbf{D}$$

$$= \left[\mathbf{K}_g^{-1} + \int_\Omega \int_\psi \frac{1}{h} (\mathbf{P} \otimes \mathbf{P} + \chi \mathbf{P} \otimes \mathbf{P} : \mathbf{K}_g^{-1}) \, d\Omega \, d\Psi \right] : \dot{\mathbf{T}}.$$

Equations (3.6) and (3.7) give two variants of the explicit form of the constitutive equation with two kinds of material parameters h and χ. The Bauschinger effect $\beta = (\tau_{cr} - \tau_{-cr})/2\tau_{cr0}$ is reflected in the activation rule of slip systems (LIANG et

al. [13]),

if $\tau = \tau_{\mathrm{cr}}$ and $\dot{\tau} > \dot{\tau}_{\text{latent}}$, then
$$\begin{cases} \dot{\gamma} > 0, \\ \dot{\tau}_{\mathrm{cr}} = \dot{\tau} = h\dot{\gamma} + \chi \mathbf{P} : \mathbf{D}^p \\ \text{and} \\ \dot{\tau}_{-\mathrm{cr}} = \dot{\tau}_{\mathrm{cr}} - 2\dot{\beta}\tau_{\mathrm{cr0}}; \end{cases}$$

(3.8)

if $\tau = \tau_{-\mathrm{cr}}$ and $\dot{\tau} < \dot{\tau}_{\text{latent}}$, then
$$\begin{cases} \dot{\gamma} < 0, \\ \dot{\tau}_{-\mathrm{cr}} = \dot{\tau} = h\dot{\gamma} + \chi \mathbf{P} : \mathbf{D}^p \\ \text{and} \\ \dot{\tau}_{\mathrm{cr}} = \dot{\tau}_{-\mathrm{cr}} + 2\dot{\beta}\tau_{\mathrm{cr0}}; \end{cases}$$

otherwise $\dot{\gamma} = 0$
$$\begin{cases} \text{if } \dot{\tau}_{\text{latent}} \geq 0, \text{ then} \begin{cases} \dot{\tau}_{\mathrm{cr}} = \chi \mathbf{P} : \mathbf{D}^p \\ \text{and} \\ \dot{\tau}_{-\mathrm{cr}} = \dot{\tau}_{\mathrm{cr}} - 2\dot{\beta}\tau_{\mathrm{cr0}}, \end{cases} \\[2em] \text{if } \dot{\tau}_{\text{latent}} < 0, \text{ then} \begin{cases} \dot{\tau}_{-\mathrm{cr}} = \chi \mathbf{P} : \mathbf{D}^p \\ \text{and} \\ \dot{\tau}_{\mathrm{cr}} = \dot{\tau}_{-\mathrm{cr}} + 2\dot{\beta}\tau_{\mathrm{cr0}}, \end{cases} \end{cases}$$

where τ_{cr} and $\tau_{-\mathrm{cr}}$ are the critical resolved shear stresses corresponding to positive and negative sliding directions, τ_{cr0} is the initial critical resolved shear stress.

It should be noticed that it is not always convenient to apply Eq. (3.6) or (3.7) directly for numerical analysis, because material parameters depend on the deformation history and the activation states of the slip systems. Usually, using the slip hardening law, Eqs. (3.3) and (3.2), yield

$$(3.9) \qquad \dot{\gamma} = \frac{\dot{\tau}}{h} - \frac{\chi}{h} \int\limits_{\Omega} \int\limits_{\Psi} (\mathbf{P} : \tilde{\mathbf{P}}) \tilde{\dot{\gamma}} \, d\Omega \, d\Psi ,$$

where the tildas mean that the corresponding variable is a function of the integral variable. Under small deformation, the above equation is a standard Fredholm integral equation with symmetric integral kernel $\mathbf{P} : \tilde{\mathbf{P}} = \tilde{\mathbf{P}} : \mathbf{P}$. If the coefficient $h > 0$, there exists one and only one solution. By dividing half of the spherical angle, orientation range of $\mathbf{n}$, into N equal parts and half of the plane angle, orientation range of $\mathbf{m}$, into M equal parts, a discrete model with MN slip systems will be obtained for numerical analysis. In this case, Eq. (3.9) becomes

$$(3.10) \qquad \dot{\gamma}^{(j)} + \frac{2\pi^2}{MN} \frac{\chi}{h^{(j)}} \sum_{i=1}^{MN} [\mathbf{P}^{(j)} : \mathbf{P}^{(i)}] \dot{\gamma}^{(i)} = \frac{1}{h^{(j)}} \dot{\tau}^{(j)}$$

(for all activated slip systems).

As far as all activated slip systems are concerned, Eq. (3.10) is a set of equations with a symmetric and positive definite coefficient matrix. However, the determination of activation state of slip systems must be combined with the activation rule of slip systems. Therefore, it is generally solved by iteration. For finite deformation, terms $\dot{\tau}^{(j)}$ of the above equations are functions of $\mathbf{D}$, so that the iteration is more complicated than that for small deformation. When all slidings are determined, the macro-stress or strain and the stiffness or compliance tensors can completely be determined.

4. Discussion of deformation-induced anisotropy

The initially isotropic assumption of a polycrystalline aggregate can be tested by macroscopic experiments as well as microscopic observations. The anisotropy that follows is then deformation-induced. Based on the material model proposed in this paper, the material element is divided into $MN = 876$ discrete slip systems.
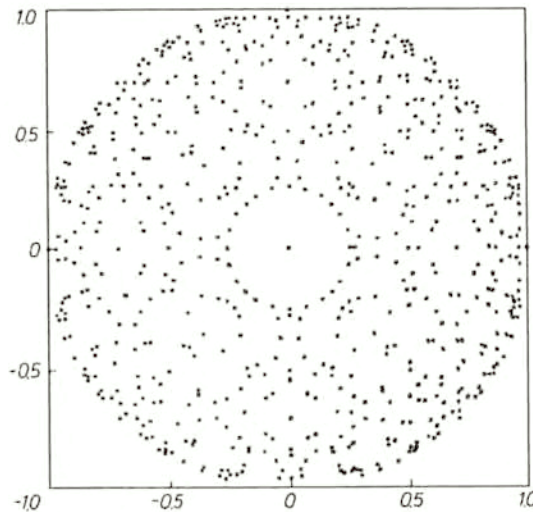

FIG. 1. The initial distribution of the discrete slip systems in the model material, here projected on a plane.

Figure 1 gives the initial distribution of the discrete slip systems in the model material, here projected on a plane. The evolution laws of the three kinds of material parameters h, χ and β included in the constitutive relation are, respectively (LIU and LIANG [13]),

(4.1) $$h = (h_0 - h_{sat})\frac{\tau_{max0} - \tau}{\tau_{max0} - \tau_{cr0}} + h_{sat},$$

(4.2) $$\chi = \chi_0 \frac{\sum |\dot{\gamma}^{(i)}| h^{(i)}}{\sum |\dot{\gamma}^{(i)}|} \qquad \text{(for all activated slip systems)},$$

(4.3) $\beta = (1 - \lambda_\beta)e^{-\alpha_\beta \Lambda^2} + \lambda_\beta$,

where $\Lambda = \int\limits_0^t \dfrac{|\max(\dot{\tau}, \dot{\tau}_\chi)|}{\tau_{cr0}} \, dt$ and $\dot{\tau}_\chi = \chi \mathbf{P} : \mathbf{D}^p$. The material constants are listed in Table 1.

Table 1. Material constants.

Material constant	Symbol	Value
Initial critical shear stress	τ_{cr0}	665 kg/cm^2
Latent hardening coefficient	χ_0	0.7
Initial hardening modulus	h_0	6916 kg/cm^2
Saturation hardening modulus	h_{sat}	5320 kg/cm^2
Nominal maximum shear stress	$\tau_{max\,0}$	798 kg/cm^2
Attendant Bauschinger coefficient	λ_β	0.8
Saturation-rate coefficient of λ_β	α_β	10

For initially isotropic materials, SZCZEPIŃSKI's [7] experiment can illustrate well the deformation-induced anisotropy on the macroscale. A sheet of an Al-2%Mg aluminium alloy, initially isotropic, was prestressed under small uniaxial tension in the x-direction until 1.92% of permanent deformation was reached. Small specimens were cut out in different directions making various angles α with the
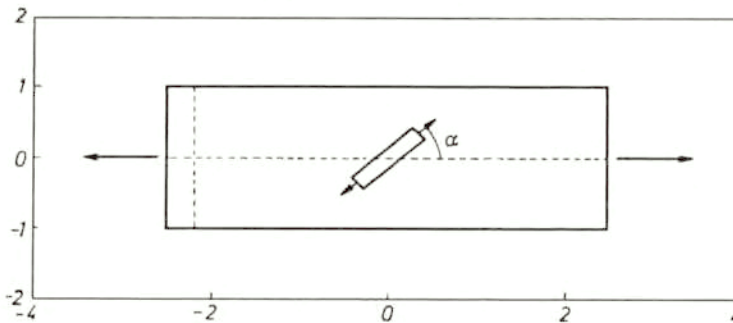

FIG. 2. The diagrammatic sketch of original specimen and small specimens.

x-axis (Fig. 2). Then all these specimens were loaded by uniaxial tensions. The experimental results show that the material evidently exhibits the Bauschinger effect, and that the consecutive yield surfaces at the prestress point possess larger curvature. The basic characteristics are the same as for other polycrystalline materials.
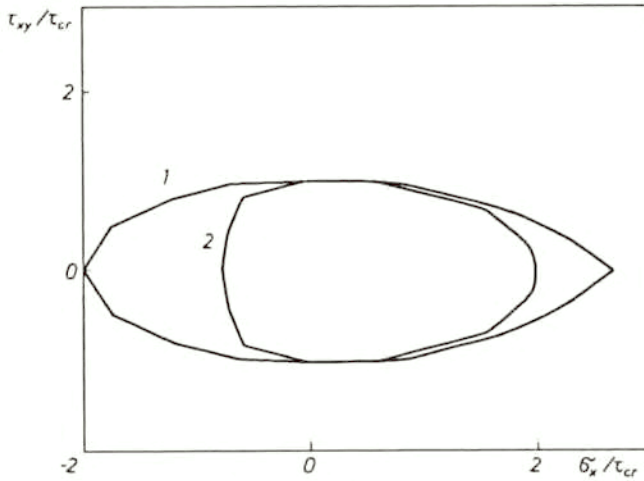
FIG. 3. Development of consecutive yield surfaces in a specimen under uniaxial tension in the x-direction. Curve (1) is the initial yield surface and (2) a subsequent yield surface.

Figure 3 shows two consecutive yield surfaces of the material measured by the proportional limit of the material. The initial yield surface is just the Tresca ellipse. The latent hardening and evident Bauschinger effect are embodied in the subsequent yield surface of the material. The change of shape of the subsequent yield surface indicates that the material behavior is far from isotropic. Figure 4
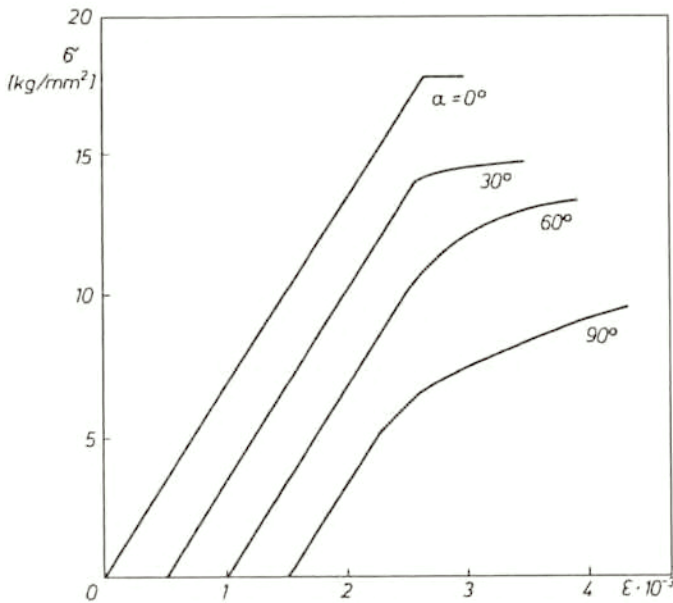

FIG. 4. Stress-strain curves in α-direction for specimens which were subjected to a permanent prestrain of 1.92% in the x-direction. α indicates the direction of the uniaxial tension relative to the x-direction.

presents tensile curves along different directions after the material underwent the 1.92% of permanent deformation. The results demonstrate that the proportional limits of the material are distinctly different in various directions. The proportional limits near $\alpha = 90°$ (perpendicular to x-axis) are mainly affected by the Bauschinger effect, and the ones near $\alpha = 0°$ mainly by the latent hardening. On the meso-scale, the change is mainly reflected in the variation of the critical resolved shear stress of the slip systems. As is well known, the critical resolved shear stress of a slip system not only depends on its activation state and deformation history, but is also affected by the interaction between the slip systems. Because
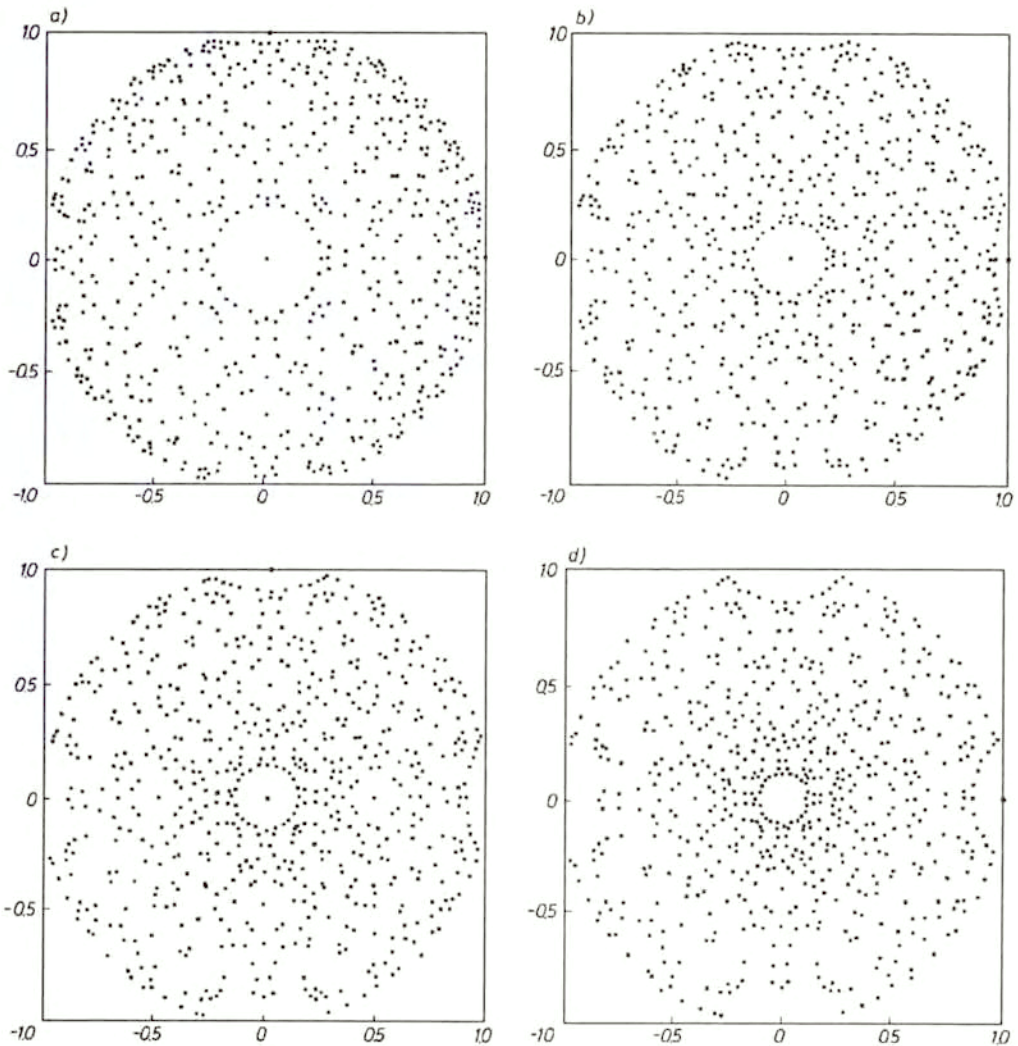

FIG. 5. Evolution of the orientation of slip systems under uniaxial tension, a) is the distribution of orientations of slip systems with a permanent prestrain of 1.92%, b), c) and d) are the distributions corresponding to 31.8%, 47.9% and 71.8% of tensile deformation, respectively.

the activation state and the deformation history are different from one slip system to another, the distinction between critical resolved shear stresses naturally results in the anisotropy measured by the macro-experiment. The evolution of consecutive yield surfaces and variation of the critical resolved shear stress under complex deformation histories have been given in reference [13] and will not be repeated here.
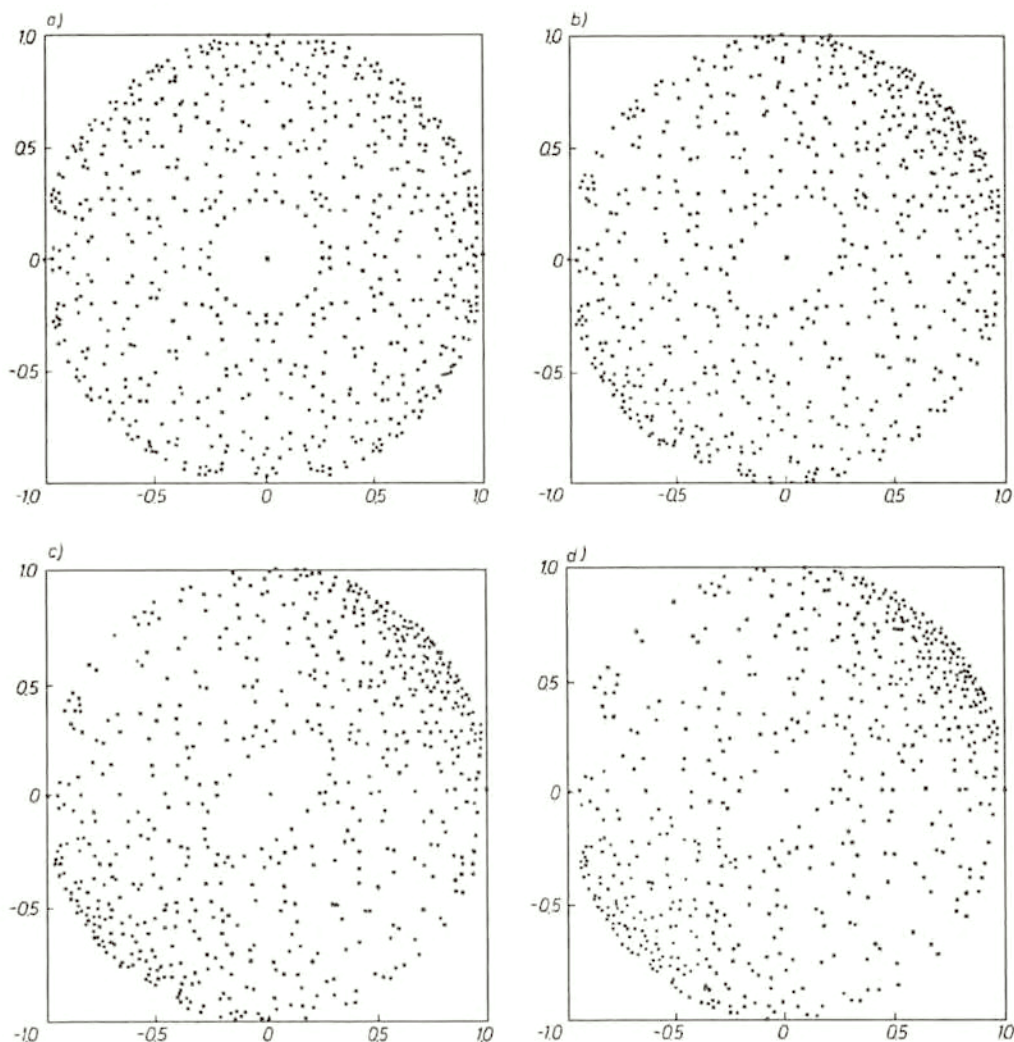
FIG. 6. Evolution of the orientations of slip systems under pure shear. (a)–(d) are the distributions corresponding to the initial distribution, 26%, 44% and 63% of shear deformation, respectively.

On the other hand, the deformation-induced anisotropy can be analyzed by the density of the orientation distribution of slip systems. Generally, the tips of

the unit sliding direction vectors **m** distributed in the 3-D space are points on the unit hemisphere, and for isotropy this distribution on this hemisphere is uniform. Figure 5a shows the distribution of the sliding orientations projected on the plane perpendicular to the tensile axis after the material underwent a 1.92% permanent tensile deformation corresponding to the above example. The variation of the sliding orientation can hardly be seen. Therefore the anisotropy discussed above is induced by the heterogeneity in the material property. However, under finite deformation, the variation of the orientation of the slip systems plays an important role in the deformation-induced anisotropy. Figure 5 b, c, d demonstrates the evolution of the orientation of the slip systems corresponding to different tensile deformation. With increasing deformation, the slip system orientations accumulate around the tensile axis. The variations of the sliding orientations under pure shear are shown in Fig. 6. With the increase of deformation, the slip system orientations accumulate around the 45° direction.

To sum up, the deformation-induced anisotropy of polycrystalline material can be divided into two kinds: one is induced by the heterogeneity of the material property due to complex deformation history, the other by the re-orientation of the slip systems or the variation of the micro-structure due to finite deformation. The meso-elastoplastic constitutive equation for finite deformation is able to predict the anisotropy mentioned above and the predicted results are in good agreement with experiments. This analysis also indicates that Szczepiński's experiment may be used as a simple and feasible method to calibrate material constants of the model with the active hardening, latent hardening and Bauschinger effect.

Acknowledgements

References

1. Th. THORSTEINSSON, *EISMINT workshop on the mechanical properties of polar ices and ice sheet modelling*, Aussois, France, January 5-7, 1994.

2. W. SZCZEPIŃSKI, Arch. Mech., **44**, 5, 663–698, 1992.

3. G. SOCHA and W. SZCZEPIŃSKI, Arch. Mech., **46**, 1, 77–190, 1994.

4. Y.F. DAFALIAS, ASME, J. Appl. Mech., **52**, 865–871, 1985.

5. Y.F. DAFALIAS, Acta Mechanica, **100**, , 171–194, 1993.

6. B. RANIECKI and Z. MRÓZ, [in:] Inelastic Solids and Structure, A. Sawczuk Memorial Volume, M. KLEIBER and A. KÖNIG [Eds.], Pineridge Press, 13–32, 1989.

7. W. SZCZEPIŃSKI, Arch. Mech. Stos., **15**, 275–296, 1963.

8. S. STEINEMANN, J. Glaciol., **2**, 16, 404–413, 1954.

9. N.M. RIBE, Geophysical J., **97**, 199–207, 1989.

10. E. VAN DER GIESSEN, Mech. Mat., **13**, 93–115, 1992.

11. B. Svendsen and K. Hutter, *On the continuum modeling of induced anisotropy in polycrystals*, Quarterly Appl. Math. [in print].

12. P. Lipinski, M. Berveiller and F. Corvasce, Arch. Mech., **40**, 725–740, 1988.

13. Liang Nai-gang, Liu Hong-qiu and Wang Zhi-chiang, The Fourth International Symposium on Plasticity and Applications, USA 1993.

14. Liu Hong-qiu and Liang Nai-gang, The First Asia-Oceania International Symposium on Plasticity, pp. 438–445, China 1993.

INSTITUTE OF MECHANICS
CHINESE ACADEMY OF SCIENCES, BEIJING, CHINA
and
INSTITUTE OF MECHANICS
TECHNISCHE HOCHSCHULE DARMSTADT, DARMSTADT, GERMANY.